





Dynamic Breath Limonene Sensing at High Selectivity

Journal Article

Author(s):

[Weber, Ines](#) ; [Oosthuizen, Dina Naude](#) ; [Mohammad, Rawan W.](#); [Mayhew, Chris A.](#); [Pratsinis, Sotiris E.](#) ; [Güntner, Andreas](#) 

Publication date:

2023

Permanent link:

<https://doi.org/10.3929/ethz-b-000622202>

Rights / license:

[In Copyright - Non-Commercial Use Permitted](#)

Originally published in:

ACS Sensors 8(7), <https://doi.org/10.1021/acssensors.3c00439>

Funding acknowledgement:

ETH-05 19-2 - Personalized indoor air quality monitoring with room-temperature filter-sensor arrays (ETHZ)
170729 - Integrated system for in operando characterization and development of portable breath analyzers (SNF)
175754 - Flame-made gas sensor arrays: Membrane-enhanced selectivity for breath analysis (SNF)

Dynamic breath limonene sensing at high selectivity

Ines C. Weber^{1,2}, Dina N. Oosthuizen¹, Rawan W. Mohammad¹, Chris A. Mayhew³, Sotiris E. Pratsinis¹, Andreas T. Güntner^{2,4*}

¹Particle Technology Laboratory, Department of Mechanical and Process Engineering, ETH Zurich, CH-8092 Zurich, Switzerland

²Department of Endocrinology, Diabetology, and Clinical Nutrition, University Hospital Zurich (USZ) and University of Zurich (UZH), CH-8091 Zurich, Switzerland

³Institute for Breath Research, Universität Innsbruck, Innsbruck A-6020, Austria

⁴Human-centered Sensor Laboratory, Department of Mechanical and Process Engineering, ETH Zurich, CH-8092 Zurich, Switzerland

Submitted to:

ACS Sensors

*corresponding author: andreas.guentner@hsl.ethz.ch

Abstract

Liver diseases (e.g., cirrhosis, liver cancer) cause more than two million deaths per year worldwide. This is partly attributed to late diagnosis and insufficient screening techniques. A promising biomarker for non-invasive and inexpensive liver disease screening is breath limonene, that can indicate a deficiency of the cytochrome P450 liver enzymes. Here, we introduce a compact and low-cost detector for dynamic and selective breath limonene sensing. It comprises a chemoresistive sensor based on Si/WO₃ nanoparticles pre-screened by a packed bed Tenax separation column at room temperature. We demonstrate selective limonene detection down to 20 parts per billion over up to three orders of magnitude higher concentrated acetone, ethanol, hydrogen, methanol and 2-propanol in gas mixtures, as well as robustness to 10 – 90% relative humidity. Most importantly, this detector recognized the individual breath limonene dynamics of four healthy volunteers following the ingestion (swallowing or chewing) of a limonene capsule. Limonene release and subsequent metabolization was then monitored from breath measurements in real-time and in excellent agreement ($R^2 = 0.98$) with high resolution proton transfer reaction mass spectrometry. This study demonstrates the potential of the detector as a simple-to-use and non-invasive device for the routine monitoring of limonene levels in exhaled breath to potentially facilitate early diagnosis of liver dysfunction.

Keywords: gas sensors, nanotechnology, liver disease, breath analysis, diagnostics, mobile health, PTR-ToF-MS

Chronic liver disease and cirrhosis accounted for 3.5% of all deaths worldwide in 2019.¹ Typically, liver disease progresses asymptotically and is detected during clinical decompensation,² such as ascites, sepsis, variceal bleeding, non-obstructive jaundice, and encephalopathy. Then, reliable diagnosis is possible with non-invasive but time consuming and expensive imaging methods³ such as ultrasound, Magnetic Resonance Elastography (MRE), Magnetic Resonance Imaging (MRI), and Computerised Tomography (CT), but these may not be readily available for many clinicians. Invasive liver biopsy is a commonly used diagnostic tool for assessing liver disease,⁴ but comes with associated risks and only samples a small volume of the liver. Whilst blood tests provide useful information on the levels of serum bilirubin and the liver enzymes alanine aminotransferase and alkaline phosphatase, they provide limited information on liver function,⁵ and levels can remain at normal values until liver decompensation occurs.⁶ Blood tests are also not specific because increased levels can arise due to, for example, acute liver injury. Owing to the asymptomatic nature of liver disease, it is estimated that more than 50% of the patients receive their diagnosis only at an advanced disease stage,² when curative treatments to stabilize disease progression are less successful. This greatly increases mortality rates.⁷ Thus, novel techniques for early-stage detection are needed.²

A promising and non-invasive⁸ tool to diagnose and monitor diseases is breath analysis.⁹ A known volatile breath marker for liver disease is d-limonene,¹⁰ a harmless exogenous monoterpene that is regularly ingested from citrus fruits,¹¹ oils,¹² cosmetics,¹³ and fragrances¹⁴ or inhaled (e.g., perfumes). There is no evidence for any endogenous production of limonene.¹⁵ Typically, limonene is metabolised to trans-carveol, trans-isopiperitenol or perillyl alcohol by the cytochrome P450 enzymes CYP2C9 and CYP2C19 in the liver.¹⁶ However, if liver function is impaired, limonene metabolization by these enzymes is reduced, which is apparent for CYP2C19 already at the earliest stage of disease.¹⁷ As a result, patients with liver cirrhosis feature elevated median limonene concentrations of 14.2 parts per billion (ppb, going up to 170 ppb¹⁰) compared to 1.5 ppb in healthy controls.¹⁵ A similar trend was observed by other studies¹⁸⁻²¹, including hepatocellular cancer patients.¹⁸ Importantly, these limonene concentrations dramatically drop in patients to 2.3 ppb within few days after liver transplantation, providing evidence that limonene is a true biomarker for liver disease.¹⁰

To differentiate between healthy and diseased metabolic functions, clinicians often apply kinetic tests, for instance, to diagnose lactose malabsorption (H₂ breath tests²²) and type 2 diabetes (oral glucose tolerance test²³). While not yet established for liver function

assessment, monitoring levels of limonene in breath, following its intake and subsequent metabolization, could serve similarly as a non-invasive kinetic test to diagnose liver disease, as well as a method to monitor the success of treatments (e.g., liver transplantation).²⁴

Towards this, a recent study has reported that administering peppermint oil capsules (which contain limonene) led to a 12-fold concentration increase in monoterpenes after 30 min and a reduction to baseline level after 285 min in the breath of healthy volunteers.¹²

Limonene has been detected in exhaled breath using various techniques such as soft chemical ionization mass spectrometric²⁰ and gas chromatography-mass spectrometric²¹ methods. Whilst these techniques are suitable for discovery programs, for clinical applications these instruments are too expensive and too bulky. More promising are compact sensors that can be integrated into handheld devices to be used by clinicians or by patients at risk of liver disease for regular screening or therapeutic monitoring.⁹ Different sensor types have been reported for the detection of limonene in breath²⁵ and food²⁶ applications, including optical (e.g., SU-8 whispering gallery mode resonator²⁷), chemoresistive (e.g., polystyrene-based molecularly imprinted polymer (MIPs) with organic semiconductor poly(3-hexylthiophene)²⁶), quartz crystal microbalance (QCM, with MIP coating²⁸ and as an array²⁵) and electrochemical (e.g., thiol-capped Au nanoparticles²⁹) sensors. However, these feature insufficient limits of detection for breath applications, with the lowest measured concentration being 6 ppm in dry air.²⁷ In addition, their selectivity towards competing breath markers (e.g., acetone, ethanol, methanol, etc.) has not been assessed.

Here, we present details on a novel detector³⁰ which comprises a separation column³⁰ followed by a highly sensitive chemoresistive³¹ sensor. Si/WO₃ was chosen due to the high sensitivity of WO₃ to terpenes³² (including d-limonene³³). The separation column restricts the transport of limonene molecules, while other breath volatiles (referred to as interferants) pass through the column essentially unhindered, allowing for sequential and hence selective detection of first the interferants and then the limonene by the sensor (**Figure 1a**). Information on the detector's selectivity and sensitivity are reported for both limonene as a single analyte and for limonene in gas mixtures containing commonly found volatiles in breath (e.g., acetone, ethanol, isoprene, carbon monoxide, hydrogen, methanol, and 2-propanol) that can have up to three orders of magnitude higher breath concentrations than limonene. The robustness of the detector to various relative humidities is also assessed. The potential of this detector is illustrated by evaluating its performance under real conditions through a series of

breath tests involving four healthy volunteers who had ingested (swallowed or chewed) a capsule containing limonene.

Experimental Section

Si/WO₃ sensor and Tenax separation column fabrication

The limonene detector consists of a highly sensitive flame-made³¹ Si/WO₃ sensor that is pre-screened³⁴ by a room temperature Tenax TA separation column (**Figure 1a**).³⁰ The sensor was produced by flame spray synthesis and direct deposition of 10 mol% Si/WO₃ nanoparticles onto interdigitated Pt electrodes on an Al₂O₃ substrate.³⁵ The sensor was mounted onto a Macor holder installed inside a Teflon chamber and heated to 300 °C by applying a constant voltage to a Pt heater that was placed on the back of the substrate (HMC803, R&S, Germany) while a multimeter (Keithley, 2700) was used to record the ohmic film resistance between the electrodes.³⁵

The separation columns were prepared using 25 mg commercial Tenax TA (poly(2,6-diphenyl-p-phenylene oxide), 60–80 mesh, ~35 m²/g, Sigma Aldrich). The powder was assembled as a packed bed inside a Teflon tube of 4 mm inner diameter and secured with quartz wool on both ends.³⁰ Prior to any measurements, the tube was flushed with 300 mL/min of dry synthetic air (C_nH_m and NO_x ≤ 100 ppb, PanGas, Switzerland) for two hours to remove possible volatile contaminants. The separation columns were connected to the sensors using inert Teflon tubing.

Sensing tests

Sensing tests were carried out with a setup described in detail elsewhere.³⁶ Using mass flow controllers (MFCs, Bronkhorst, Netherlands), the analytes d-limonene (17 ppm, in dry synthetic air, PanGas), acetone (15 ppm), methanol (504 ppm), 2-propanol (200 ppm), hydrogen (50 ppm), carbon monoxide (CO, 500 ppm), ethanol (15 ppm), and isoprene (500 ppm) were dosed into high purity dry synthetic air. The relative humidity (RH) of these calibration standards was adjusted to 10 – 90% by linearly ad-mixing an air stream that was bubbled through ultrapure water (Milli-Q A10, Merck, Switzerland) and validated with a humidity sensor (Sensirion, SHT2x), which was used also to measure the ambient air temperature and RH. The total flow rate was set at 300 mL/min. The detector was evaluated for single analytes and mixtures for 180 s exposures (unless mentioned otherwise). Sensing tests were performed with and without the Tenax separation column upstream of the sensor.

Breath measurements

Breath measurements were carried out with four female volunteers aged 25 – 34. All were healthy, i.e., without known liver, kidney, cardiovascular, or respiratory diseases. Also, these volunteers were non-smoking and had abstained from alcohol and chemical mouthwash for, at least, 12 hours prior to these measurements. Drinking (except water) and eating was not allowed throughout the breath study to minimize any interference from confounding volatiles.

Breath exhalations were carried out using a tailor-made end-tidal breath sampler³⁷ with a tube volume of 270 mL and a flow restrictor to allow for controlled breath exhalations. The volunteers were asked to exhale completely into that sampler through a sterile and removable mouthpiece (EnviteC-Wismar GmbH, Germany) for about 30 s. The exhaled breath gas was analyzed simultaneously with the detector (i.e., the Si/WO₃ sensor pre-screened by the Tenax separation column) and a proton-transfer-reaction time-of-flight mass spectrometer (PTR-ToF-MS 1000, Ionicon Analytik GmbH, Austria), which has a high mass resolving power of up to 1000 $m/\Delta m$. A diaphragm pump (SP 270 EC-LC, 5 V DC, Schwarzer Precision, Germany) was used to maintain a constant gas flow of 300 mL/min, which drew the breath sample into the drift tube (reaction region) of the PTR-ToF-MS. The flow rate was validated by a calibrated flow meter at the pump outlet.

For this study, the drift tube of the PTR-ToF-MS was connected downstream of the breath sampler and the detector through inert Teflon tubing that was heated to avoid condensation. Descriptions of the key operating principles and general details of PTR-ToF-MS applications are provided in depth in the literature.³⁸ In brief, the drift tube of the PTR-ToF-MS was operated at a voltage of 600 V and maintained at a temperature of 60 °C and a pressure of 2.3 mbar. The H₃O⁺ primary ions were produced via a series of ion-molecule reactions in a hollow cathode discharge ion source containing water vapor originating from a reservoir of pure water. Upon transfer into the detection region of the instrument, the reagent and product ions were separated in the drift tube according to their drift times and detected with a multichannel plate detector. Drift times of the ions were converted to m/z values through mass calibration. Reactions of H₃O⁺ with limonene in the drift tube are known to produce two dominant product ions at mass-to-charge ratios m/z 137.13, C₁₀H₁₇⁺ (non-dissociative proton transfer) and m/z 81.07, C₆H₉⁺ (dissociative proton transfer).¹² For this study the signal intensity of C₁₀H₁₇⁺ was sufficient to determine accurately breath concentrations.

Study design

The study protocol started with a single breath exhalation to provide the background level of limonene in a volunteer's breath. This was followed by the consumption of a d-limonene soft gel capsule (Jarrow Formulas) that contained 1000 mg of limonene enclosed in a bovine gelatin shell. Whereas volunteer #1 was asked to swallow the capsule, volunteers #2, #3 and #4 were asked to chew it first before swallowing to accelerate limonene release. After chewing and ingestion, volunteers #2, #3 and #4 were asked to rinse their mouths to remove potential limonene residuals in their oral cavities. Breath exhalations were analyzed every 30 min for volunteer #1. For volunteers #2, #3 and #4, breath exhalations were analyzed 15 min after limonene consumption (to capture rapid limonene dynamics), followed by 30-min intervals. This study was not subject to ethics approval, as confirmed by the ETH Zurich Ethics Commission. However, each volunteer gave written informed consent prior to the tests.

Data analysis

The response (S) of a sensor is defined as:

$$S = \frac{R_{air}}{R_{analyte}} - 1,$$

with R_{air} and $R_{analyte}$ being the sensing film resistances in air and during analyte exposure, respectively. The sensor selectivity is defined as the ratio of the limonene response to the interferant response according to IUPAC guidelines.³⁹ The signal-to-noise ratio (SNR) represents the ratio of the film resistance change by analyte exposure over baseline fluctuations, i.e., the standard deviation in air, as determined over, at least, 20 data points. The response time is defined as the time needed to reach 90% of the resistance change. The retention time (t_r) is defined as the time from the start of the exposure to the maximum response.⁴⁰ To evaluate the breath measurements, the limonene sensor response is calculated at a fixed retention time of 150 s. Only at high limonene concentrations, where the signal of limonene and retained species overlaps, the maximum sensor response was used.

For the PTR-ToF-MS measurements, analyte concentrations were determined at m/z values of 33.03 (methanol⁴¹), 59.05 (acetone⁴²), 69.07 (isoprene⁴¹), and 137.13 (limonene¹²) by integrating over the peak area using the PTR-MS Viewer 3.1 software. Breath limonene concentrations were calculated at the maximum dynamic signal intensity by comparing to three-point calibrations that were carried out with the Tenax separation column over the relevant range, using the above calibration gas standard.

Experimental measurements were repeated at least three times from which the average value and standard deviation (σ) was calculated. The sample size (N) is indicated in the figure legends for each statistical analysis. The coefficient of determination (R^2) and Pearson correlation coefficient (r_p) were calculated to determine the variation and linearity between two data sets, respectively. For breath evaluation, limonene levels were normalized to the maximum values detected for better comparison of limonene uptake and metabolism dynamics between individual volunteers.

Results and Discussion

Selective limonene detection

Figure 1b shows the response of a Si/WO₃ sensor without the separation column upon exposure to 100 ppb limonene (blue, solid line) and 1000 ppb acetone (purple, dashed line), 2-propanol (brown), methanol (green) and hydrogen (red) at 50% RH. The latter four compounds were chosen because they are typical breath interferants that can occur at elevated concentrations in healthy volunteers (e.g., > 1.5 ppm methanol,⁴³ > 0.1 ppm 2-propanol,⁴⁴ > 10 ppm hydrogen⁴⁵ and > 2.5 ppm acetone⁴⁴). The sensor responds quickly to the analytes (i.e., within 12 s for limonene) through a change in electrical resistance that is considered to occur as a result of the interaction of an analyte with oxygen vacancies and/or ionosorbed surface species that alter the charge carrier concentration and mobility in the surface-near layers, typical for WO₃-based chemoresistive sensors.⁴⁶ The highest sensor response is observed for limonene (i.e., 1.92), followed by acetone (1.65) and 2-propanol (0.36). Methanol and hydrogen are hardly detected (response < 0.1), in agreement with literature.⁴⁷ However, this sensor cannot discriminate these analytes, which is typical⁴⁸ for such chemoresistive sensors. While high sensor responses towards acetone have been reported for Si/WO₃ sensors,³⁵ the higher response to the much lower concentrations of limonene is remarkable. This is in agreement with previous works showing higher responses for terpenes³² (e.g., d-limonene³³) for WO₃-based sensors when compared to In₂O₃ and ZnO.³³

Selective limonene detection is enabled by placing the Tenax separation column ahead of the sensor, with the limonene peak occurring now at a retention time of 315 s (solid line, 100 ppb, **Figure 1c**), while all interferants (dotted lines) pass through the column essentially unscathed and their detection is terminated after 240 s. Most importantly, the limonene peak does not overlap with the interferants' responses. Note that limonene retention comes with a response reduction from 1.92 without the separation column to 0.39 with the separation

column at 100 ppb, while the unhindered acetone and 2-propanol reach almost identical responses (deviations < 5%), as expected.³⁰ Similarly, various other critical breath interferants, such as ethanol and isoprene, remain unaffected by the separation column, while the responses are generally low for hydrogen, methanol, and CO, as reproducibly shown for three identically prepared detector systems (error bars, **Figure S1**).

The limonene retention is attributed to the Tenax particles that feature high surface area (25 m²/g)⁴⁹ and separate molecules predominantly by unspecific adsorption through van der Waals forces.⁵⁰ Hence, heavier molecules such as limonene (136.24 g/mol) are retained longer, and feature higher breakthrough volumes (e.g., 12000 L/g at 20 °C⁵¹) than interfering molecules (e.g., 0.36, 5.0, and 6.0 L/g for methanol, 2-propanol and acetone at 20 °C, respectively⁵¹). It is worth noting that the retention characteristics can be adjusted through the Tenax loading in the packed bed and the gas flow rate.³⁴ This has been demonstrated for selective methanol (in breath³⁰ and hand sanitizers⁵²) and formaldehyde⁴⁹ detection, even as an integrated device.⁵³

In exhaled breath, limonene concentrations can vary, thus the detector was tested from 20 to 500 ppb (**Figure 1c** and its inset). Most importantly, 20 ppb of limonene were detected with a SNR of 6.3 and clearly distinguished from the interferants. This outperforms sensors that measured, at best, only 6 ppm (SU-8 whispering gallery mode resonator²⁷), 50 ppm (polystyrene-based molecularly imprinted polymers (MIPs) and organic semiconductor poly(3-hexylthiophene)²⁶), and 113 ppm (thiol-capped Au nanoparticles²⁹) of limonene. Note that the retention time is rather constant for small limonene concentrations (i.e., 330 ± 11 s between 20 and 100 ppb), but decreases at higher levels (down to 253 s at 500 ppb, **Figure S2**), in line with literature.³⁰ While the detector requires more than 15 min to regenerate to its initial baseline, this can be improved by slight heating (e.g., raising the temperature to 80 °C⁵⁴) or by switching the filter,⁵⁵ if required. Note that the ambient air temperature in the controlled laboratory environment was maintained at 23.7 ± 1.2 °C. In case of larger temperature variations, the detector may be equipped with an additional temperature sensor that corrects for temperature-related retention time changes³⁰ in the separation column.

Exhaled breath is a complex gas mixture that can contain more than 1000 volatiles.⁵⁶ Hence, the detector's performance is assessed for 50, 75 and 100 ppb limonene together with the interferants acetone, methanol, 2-propanol and hydrogen (each at 1000 ppb, **Figure 1d**, dashed line). Clearly, the detector measures first the interferants followed by the limonene. Its peak is nearly identical in the gas mixture compared to that as a single analyte (solid line) for

all limonene concentrations ranging from 20 ppb up to 500 ppb, with a high coefficient of determination, $R^2 > 0.999$ between single analyte and gas mixture measurements (**Figure 1e**). A linear response relation holds over the entire concentration range, as expected for such Si/WO₃ sensors at low analyte concentrations.³¹ The high limonene sensitivity and selectivity are unprecedented (to the best of our knowledge), and are enabled by the flame-aerosol deposited, nanostructured sensor⁵⁷ and the separation column, respectively. Without it, the sensor would greatly overestimate the limonene concentration in that gas mixture (**Figure S3**, squares).

The selectivity of the separation column is maintained even in gas mixtures containing orders of magnitude higher breath-relevant concentrations of acetone (up to 4 ppm⁵⁸), H₂ (up to 20 ppm⁴⁵), and ethanol (up to 100 ppm⁵⁹), which may be present in breath from alcohol intake or inhaling hand disinfection or cleaning agents. In fact, the response to 100 ppb limonene is hardly affected by these interferants (< 20%, **Figure 2**) compared to single analyte (dashed line). Note that the normalized response is shown here to better visualize the relative error. This demonstrates that the detector is quite robust to extreme conditions that may be present in environments such as hospitals or clinics. Finally, it also features excellent repeatability (i.e., < 3% deviation, **Figure S4**), making it attractive for precise and repeatable limonene sensing.

Humidity robustness

Relative humidity varies significantly in indoor and outdoor air (e.g., 32 – 84% RH⁶⁰) and reaches more than 90% in exhaled breath.⁶¹ Hence, the detector was challenged further at 90, 70, 50, 30, and 10% RH while exposing it to 100 ppb limonene together with a gas mixture containing acetone, methanol, 2-propanol and hydrogen, each at 1000 ppb. The detector resistance is shown in **Figure 3a**. With decreasing RH, the baseline resistance drops from 24 to 20 MΩ at 90 (i.e., close to exhaled breath) and 30% RH (laboratory air, **Figure S5**), respectively. This has been associated with the reaction of water molecules with oxygen vacancies on the WO₃ surface.⁴⁶ It corresponds to a detector response of 0.2, that is similar to 60 ppb of limonene (Figure 1e), that did not compromise dynamic limonene monitoring, as will be shown later. Most importantly, RH variations do not affect limonene selectivity by the separation column. In fact, the limonene peak occurs at almost identical retention times (< 5% variation for all RH), suggesting minimal RH influence, in line with literature.⁵⁴ Remarkably,

the detector response to 100 ppb limonene for all RH (considering their individual baselines) hardly changes (i.e., 0.36 ± 0.012 , **Figure 3b**), indicating high RH robustness.

Limonene detection in breath

To demonstrate the detector's potential for breath analysis, it was tested on four volunteers, with the protocol for volunteer #1 shown in **Figure 4a**. This protocol was chosen as it is a promising tool to assess liver function by tracking limonene uptake and decline, which reflects the rate of metabolization. **Figure 4b** shows the detector response to the breath exhalation at 0 min of volunteer #1 prior to limonene administration (solid line, top). The detector responds quickly (i.e., within 26 s, with a maximum response of 2.3) and fully recovers the baseline after about 150 s. This response is attributed to non-retained breath molecules, in agreement with Figure 1b,c, and is validated exemplarily by PTR-ToF-MS measurements (dashed lines, bottom) for acetone (1.7 ppm), isoprene (0.4 ppm) and methanol (0.4 ppm).

As expected for healthy volunteers,¹⁵ hardly any limonene is detected prior to consumption of the capsule (bottom Figure 4b, right ordinate). This is similar to 60 min after limonene consumption (**Figure 4c**), where the limonene concentration remains low, probably due to delayed release from the swallowed capsule, as the bovine gelatin shell had to dissolve first. Most importantly, the absence of a response at longer retention times indicates also that other compounds with similar breakthrough volumes (e.g., octanal has 12500 L/g on Tenax at 20 °C⁵¹) do not interfere with limonene sensing, probably due to their lower concentration (median breath octanal level is 1.5 ppb⁶²) than limonene, as shown below. Worthy of note, acetone concentrations continuously increased throughout the measurements from 1.7 at $t = 0$ min to 2.5 ppm at 60 min and 4.0 ppm at 330 min, which is almost certainly due to prolonged fasting that resulted in enhanced lipolysis.⁵⁸ This suggests that acetone is a major contributor to the non-retained detector response, in agreement with Figure 1b,c. Note that differences in exposure, response and recovery times of the detector compared to the flow-bench measurements (Figure 1c) are attributed to the buffered end-tidal breath sampling procedure.³⁷

In contrast, after 210 min, the response profile is significantly altered (**Figure 4d**). Now, a response hump appears after 150 s (max. response = 2.3). This is attributed to the presence of 630 ppb limonene, as determined by the PTR-ToF-MS which detects limonene after the same retention time. Note that the shorter retention time here compared to Figures 1 and 3 (i.e., 84 s vs. 180 s exposure time, **Figure S6**) is again attributed to the different sampling, as

well as higher concentrations of limonene (**Figure 1c** and **S2**). The presence of limonene in the breath indicates release from the capsule in the stomach, which enters breath either directly from the digestive tract through the oesophagus,⁶³ or through the diffusive exchange with blood in the lung alveoli.⁶⁴ The limonene response hump increases even further after 330 min (i.e., 3.8), which is in line with the higher limonene concentration of 1062 ppb measured by PTR-ToF-MS (**Figure 4e**). Hence, the detector can follow closely changing limonene concentrations in real breath samples (see **Figure S7** for all times). More specifically, the detector response and limonene concentration by PTR-ToF-MS correlate linearly (Pearson $r_p > 0.99$, **Figure S8**), that is in good agreement with the laboratory gas mixture tests (Figure 1e). Note that each breath measurement shows a small response increase after 300 s (see Figure 4 and Figure S7), which may be attributed to water desorption from the breath sampler.

Dynamic limonene monitoring

To evaluate the effect of limonene administration and subsequent metabolization, the measured detector response (at $t = 150$ s) and maximum concentrations (PTR-ToF-MS) are shown in **Figure 5a** for volunteers #1 – 4. Note that both detector response (solid lines) and PTR-ToF-MS measured intensities (dashed lines) are normalized to the maximum signal to easily compare the increase and the decrease of limonene levels as potential indicator of liver function. Full response, limonene, isoprene, and acetone profiles are provided also for volunteers #2 - 4 in **Figures S9 – S11** for completeness.

Volunteer #1 shows delayed increase in limonene concentration (Fig. 5a, triangles) starting at 120 min, as traced by the detector in good agreement with the PTR-ToF-MS results. The maximum occurs after 270 min (concentration 1.7 ppm, Figure S7), before the limonene level decreases to 34% after 390 min (i.e., 120 min after maximum) suggesting its metabolization by liver enzymes. In contrast, when chewing the capsule (to trigger rapid limonene release into the digestive tract, volunteers #2, #3 and #4), the limonene reaches a maximum already after 15 – 75 min. Still, the subsequent limonene decrease occurs at a similar rate, for example down to 23% for volunteer #4 after 165 min (i.e., 140 min after its maximum at 15 min). This is in line with kinetic tests performed with liquid limonene administration in healthy volunteers,⁶⁵ where a maximum intensity is observed after 30 min, which dropped to approximately 5% after 180 min (i.e., 150 min after the maximum).⁵⁴

Most importantly, the detector agrees well with the levels recorded by the PTR-ToF-MS. This is illustrated in **Figure 5b**, showing a scatter plot of the normalized limonene intensity as

detected by the detector and the PTR-ToF-MS. All data points are close to the ideal dashed line, and the coefficient of determination (R^2) is 0.98 for 40 breath samples, without significant interference by other breath compounds. Hence, the detector captures accurately the individual limonene dynamics in healthy volunteers.

Conclusions

A highly sensitive and selective detector for ppb-level limonene sensing in breath has been presented. It comprises of a Tenax TA separation column which retains limonene longer than key breath interferants, and a Si/WO₃ sensor which quantifies limonene down to 20 ppb at high RH (i.e., up to 90%), outperforming state-of-the-art optical, chemoresistive and mass-sensitive sensors and arrays. High selectivity and humidity robustness is preserved in gas mixtures containing orders of magnitude higher interferant concentrations. Validated in exhaled breath from healthy volunteers, this detector accurately measures limonene concentrations, in good agreement with those determined from the PTR-ToF-MS measurements. As a result, it captures slow and rapid limonene release and metabolism in four healthy volunteers following the ingestion (swallowing or chewing) of a limonene capsule.

As a result of this proof-of-principle investigation, this detector is ready to be tested on patients with liver dysfunction in a follow-up study, however, this requires larger cohorts and ethical permission. Ideally, the detector will be integrated into a hand-held⁵³ device with wireless smartphone read-out. Based on its compact design, low-cost, and high accuracy, we envision future application of such detectors for routine and non-invasive liver dysfunction assessment, potentially capable of recognizing liver abnormalities at an early stage.

Acknowledgement

This study was mainly supported by the ETH Research Grant (ETH-05 19-2) and partially by the BRIDGE Proof of Concept grant (40B1-0_205898, SNF and Innosuisse), Swiss National Science Foundation (R'Equip grant 170729 and grant 175754), Swiss State Secretariat for Education, Research and Innovation (SERI) under contract number MB22.00041 (ERC-STG-21 "HEALTHSENSE") and the Stiftung Accentus – Verena Guggisberg-Lüthi Fonds.

Contribution

Ines C. Weber: Conceptualization, Methodology, Formal analysis, Investigation, Writing – original draft, Writing – review & editing, Visualization, Funding acquisition. *Dina N.*

Oosthuizen: Formal analysis, Investigation, Writing – review & editing, Visualization. *Rawan*

R. Mohammad: Methodology, Formal analysis, Investigation, Visualization. *Chris A.*

Mayhew: Methodology, Investigation, Writing – review & editing. *Sotiris E. Pratsinis*:

Methodology, Investigation, Writing – review & editing, Visualization, Supervision, Funding acquisition. *Andreas T. Güntner*: Conceptualization, Methodology, Formal analysis,

Investigation, Writing – review & editing, Visualization, Supervision, Funding acquisition.

Supporting information

Available: The following files are available free of charge. Sensor response to various volatiles with and without separation column (Figure S1); Retention time as a function of limonene concentration (Figure S2); Sensor response to gas mixtures with and without separation column (Figure S3); Repeatability (Figure S4); Laboratory RH and temperature (Figure S5); Effect of limonene exposure time (Figure S6); Detector and PTR-ToF-MS profiles of volunteer #1 (Figure S7); Scatter plot of detector response vs. PTR-ToF-MS limonene concentration (Figure S8); Detector and PTR-ToF-MS profiles of volunteer #2 (Figure S9); Detector and PTR-ToF-MS profiles of volunteer #3 (Figure S10); Detector and PTR-ToF-MS profiles of volunteer #4 (Figure S11).

References

1. Asrani, S. K., Devarbhavi, H., Eaton, J. & Kamath, P. S. Burden of liver diseases in the world. *J Hepatol* **70**, 151–171 (2019).
2. Tsochatzis, E. A., Bosch, J. & Burroughs, A. K. Liver cirrhosis. *The Lancet* **383**, 1749–1761 (2014).
3. Yeom, S. K., Lee, C. H., Cha, S. H. & Park, C. M. Prediction of liver cirrhosis, using diagnostic imaging tools. *World J Hepatol* **7**, 2069–2079 (2015).
4. Rockey, D. C., Caldwell, S. H., Goodman, Z. D., Nelson, R. C. & Smith, A. D. Liver biopsy. *Hepatology* **49**, 1017–1044 (2009).
5. Sherwood, P., Lyburn, I., Vrown, S. & Ryder, S. How are abnormal results for liver function tests dealt with in primary care? Audit of yield and impact. *BMJ* **322**, 276–278 (2001).
6. Cuperus, F. J. C., Drenth, J. P. H. & Tjwa, E. T. Mistakes in liver function test abnormalities and how to avoid them. *United European Gastroenterol J* **17**, 1–5 (2017).
7. D’Amico, G., Garcia-Tsao, G. & Pagliaro, L. Natural history and prognostic indicators of survival in cirrhosis: A systematic review of 118 studies. *J Hepatol* **44**, 217–231 (2006).
8. Beauchamp, J., Davis, C. E. & Pleil, J. D. *Breathborne Biomarkers and the Human Volatilome*. (Elsevier, 2020).
9. Güntner, A. T., Abegg, S., Königstein, K., Gerber, P. A., Schmidt-Trucksäss, A. & Pratsinis, S. E. Breath Sensors for Health Monitoring. *ACS Sens* **4**, 268–280 (2019).
10. Fernández del Río, R., O’Hara, M. E., Holt, A., Pemberton, P., Shah, T., Whitehouse, T. & Mayhew, C. A. Volatile Biomarkers in Breath Associated With Liver Cirrhosis - Comparisons of Pre- and Post-liver Transplant Breath Samples. *EBioMedicine* **2**, 1243–1250 (2015).
11. Negro, V., Mancini, G., Ruggeri, B. & Fino, D. Citrus waste as feedstock for bio-based products recovery: Review on limonene case study and energy valorization. *Bioresour Technol* **214**, 806–815 (2016).
12. Malásková, M., Henderson, B., Chellayah, P. D., Ruzsanyi, V., Mochalski, P., Cristescu, S. M. & Mayhew, C. A. Proton transfer reaction time-of-flight mass spectrometric measurements of volatile compounds contained in peppermint oil capsules of relevance to real-time pharmacokinetic breath studies. *J Breath Res* **13**, 046009 (2019).

13. Ciriminna, R., Rodriguez, M. L., Carà, P. D., Sanchez, J. A. L. & Pagliaro, M. Limonene: A versatile chemical of the bioeconomy. *Chem Commun* **50**, 15288–15296 (2014).
14. Sun, J. D-Limonene: Safety and clinical applications. *Altern Med Rev* **12**, 259–264 (2007).
15. O’Hara, M. E., Río, R. F. Del, Holt, A., Pemberton, P., Shah, T., Whitehouse, T. & Mayhew, C. A. Limonene in exhaled breath is elevated in hepatic encephalopathy. *J Breath Res* **10**, 46010 (2016).
16. Miyazawa Mitsuo, Masaki, S. & Tsutomu, S. Metabolism of (+)- and (–)-Limonenes to Respective Carveols and Perillyl Alcohols by CYP2C9 and CYP2C19 in Human Liver Microsomes. *Drug Metab. Dispos* **30**, 602–607 (2002).
17. Frye, R. F., Zgheib, N. K., Matzke, G. R., Chaves-Gnecco, D., Rabinovitz, M., Shaikh, O. S. & Branch, R. A. Liver disease selectively modulates cytochrome P450-mediated metabolism. *Clin Pharmacol Ther* **80**, 235–245 (2006).
18. Ferrandino, G., Orf, I., Smith, R., Calcagno, M., Thind, A. K., Debiram-Beecham, I., Williams, M., Gandelman, O., de Saedeleer, A., Kibble, G., Lydon, A. M., Mayhew, C. A., Allsworth, M., Boyle, B., van der Schee, M. P., Allison, M., Hoare, M. & Snowdon, V. K. Breath Biopsy Assessment of Liver Disease Using an Exogenous Volatile Organic Compound-Toward Improved Detection of Liver Impairment. *Clin Transl Gastroenterol* **11**, e00239 (2020).
19. Ferrandino, G., De Palo, G., Murgia, A., Birch, O., Tawfike, A., Smith, R., Debiram-Beecham, I., Gandelman, O., Kibble, G., Lydon, A. M., Groves, A., Smolinska, A., Allsworth, M., Boyle, B., van der Schee, M. P., Allison, M., Fitzgerald, R. C., Hoare, M. & Snowdon, V. K. Breath Biopsy[®] to Identify Exhaled Volatile Organic Compounds Biomarkers for Liver Cirrhosis Detection. *J Clin Transl Hepatol* **11**, 638-648 (2023).
20. Morisco, F., Aprea, E., Lembo, V., Fogliano, V., Vitaglione, P., Mazzone, G., Cappellin, L., Gasperi, F., Masone, S., De Palma, G. D., Marmo, R., Caporaso, N. & Biasioli, F. Rapid ‘Breath-Print’ of Liver Cirrhosis by Proton Transfer Reaction Time-of-Flight Mass Spectrometry. A Pilot Study. *PLoS One* **8**, e59658 (2013).
21. Friedman, M. I., Preti, G., Deems, R. O., Friedman, L. S., Munoz, S. J. & Maddrey, W. C. Limonene in expired lung air of patients with liver disease. *Dig Dis Sci* **39**, 1672–1676 (1994).
22. Ghoshal, U. C. How to Interpret Hydrogen Breath Tests. *J Neurogastroenterol Motil* **17**, 312–317 (2011).

23. Jagannathan, R., Neves, J. S., Dorcely, B., Chung, S. T., Tamura, K., Rhee, M. & Bergman, M. The oral glucose tolerance test: 100 years later. *Diabetes Metab Syndr Obes* **13**, 3787–3805 (2020).
24. Taner, T. Liver transplantation: Rejection and tolerance. *Liver Transplant* **23**, 85–88 (2017).
25. Hawari, H. F., Samsudin, N. M., Ahmad, M. N., Shakaff, A. Y. M., Ghani, S. A., Wahab, Y., Za'aba, S. K. & Akitsu, T. Array of MIP-Based Sensor for Fruit Maturity Assessment. *Procedia Chem* **6**, 100–109 (2012).
26. Völkle, J., Kumpf, K., Feldner, A., Lieberzeit, P. & Fruhmann, P. Development of conductive molecularly imprinted polymers (cMIPs) for limonene to improve and interconnect QCM and chemiresistor sensing. *Sens Actuators B Chem* **356**, 131293 (2022).
27. Lemieux-Leduc, C., Guertin, R., Bianki, M.-A. & Peter, Y.-A. Gas sensing with SU-8 whispering gallery mode resonators. *2018 International Conference on Optical MEMS and Nanophotonics (OMN)* 115–116 (2018).
28. Wen, T., Nie, Q., Han, L., Gong, Z., Li, D., Ma, Q., Wang, Z., He, W., Wen, L. & Peng, H. Molecularly imprinted polymers-based piezoelectric coupling sensor for the rapid and nondestructive detection of infested citrus. *Food Chem* **387**, 132905 (2022).
29. Nazir, N. U., Abbas, S. R., Nasir, H. & Hussain, I. Electrochemical sensing of limonene using thiol capped gold nanoparticles and its detection in the real breath sample of a cirrhotic patient. *J Electroanal Chem* **905**, 115977 (2022).
30. Van den Broek, J., Abegg, S., Pratsinis, S. E. & Güntner, A. T. Highly selective detection of methanol over ethanol by a handheld gas sensor. *Nat Commun* **10**, 4220 (2019).
31. Righettoni, M., Tricoli, A. & Pratsinis, S. E. Si:WO₃ sensors for highly selective detection of acetone for easy diagnosis of diabetes by breath analysis. *Anal Chem* **82**, 3581–3587 (2010).
32. Jisha, P., Suma, M. S. & Murugendrappa, M. v. Synthesis and characterization of WO₃-doped polyaniline to sense biomarker VOCs of Malaria. *Appl Nanosci* **11**, 29–44 (2021).
33. Kadosaki, M., Sakai, Y., Tamura, I., Matsubara, I. & Itoh, T. Development of an oxide semiconductor thick film gas sensor for the detection of total volatile organic compounds. *Electron Commun Jpn* **93**, 34–41 (2010).
34. van den Broek, J., Weber, I. C., Güntner, A. T. & Pratsinis, S. E. Highly selective gas sensing enabled by filters. *Mater Horiz* **8**, 661–684 (2021).

35. Righettoni, M., Tricoli, A., Gass, S., Schmid, A., Amann, A. & Pratsinis, S. E. Breath acetone monitoring by portable Si:WO₃ gas sensors. *Anal Chim Acta* **738**, 69–75 (2012).
36. Güntner, A. T., Righettoni, M. & Pratsinis, S. E. Selective sensing of NH₃ by Si-doped α -MoO₃ for breath analysis. *Sens Actuators B Chem* **223**, 266–273 (2016).
37. Schon, S., Theodore, S. J. & Güntner, A. T. Versatile breath sampler for online gas sensor analysis. *Sens Actuators B Chem* **273**, 1780–1785 (2018).
38. Ellis, A. M. & Mayhew, C. A. *Proton Transfer Reaction Mass Spectrometry: Principles and Applications*. (Wiley, 2013).
39. McNaught A. D. & Wilkinson A. *IUPAC. Compendium of Chemical Terminology, 2nd ed. (the 'Gold Book')*. (Blackwell Scientific Publications, 1997).
40. Geankoplis, C. J. *Transport Processes and Separation Process Principles*. (Prentice Hall, 2003).
41. Müller, M., Mikoviny, T., Feil, S., Haidacher, S., Hanel, G., Hartungen, E., Jordan, A., Märk, L., Mutschlechner, P., Schottkowsky, R., Sulzer, P., Crawford, J. H. & Wisthaler, A. A compact PTR-ToF-MS instrument for airborne measurements of volatile organic compounds at high spatiotemporal resolution. *Atmos Meas Tech* **7**, 3763–3772 (2014).
42. Schwarz, K., Pizzini, A., Arendacká, B., Zerlauth, K., Filipiak, W., Schmid, A., Dzien, A., Neuner, S., Lechleitner, M., Scholl-Bürgi, S., Miekisch, W., Schubert, J., Unterkofler, K., Witkovský, V., Gastl, G. & Amann, A. Breath acetone - Aspects of normal physiology related to age and gender as determined in a PTR-MS study. *J Breath Res* **3**, 27003 (2009).
43. Turner, C., Španěl, P. & Smith, D. A longitudinal study of methanol in the exhaled breath of 30 healthy volunteers using selected ion flow tube mass spectrometry, SIFT-MS. *Physiol Meas* **27**, 637–648 (2006).
44. Turner, C., Španěl, P. & Smith, D. A longitudinal study of ammonia, acetone and propanol in the exhaled breath of 30 subjects using selected ion flow tube mass spectrometry, SIFT-MS. *Physiol Meas* **27**, 321–337 (2006).
45. Calloway, D. J., Murphy, E. L. & Bauer, D. Determination of lactose intolerance by Breath Analysis. *Am J Dig Dis* **14**, 811–815 (1969).
46. Staerz, A., Berthold, C., Russ, T., Wicker, S., Weimar, U. & Barsan, N. The oxidizing effect of humidity on WO₃ based sensors. *Sens Actuators B Chem* **237**, 54–58 (2016).

47. Weber, I. C., Braun, H. P., Krumeich, F., Güntner, A. T. & Pratsinis, S. E. Superior Acetone Selectivity in Gas Mixtures by Catalyst-Filtered Chemoresistive Sensors. *Advanced Science* **7**, 2001503 (2020).
48. Weber, I. C. & Güntner, A. T. Catalytic filters for metal oxide gas sensors. *Sens Actuators B Chem* **356**, 131346 (2022).
49. van den Broek, J., Cerrejon, D. K., Pratsinis, S. E. & Güntner, A. T. Selective formaldehyde detection at ppb in indoor air with a portable sensor. *J Hazard Mater* **399**, 123052 (2020).
50. Schneider, M. & Goss, K. U. Systematic investigation of the sorption properties of tenax TA, chromosorb 106, porapak N, and carbopak F. *Anal Chem* **81**, 3017–3021 (2009).
51. Scientific Instrument Services. Tenax® TA Breakthrough Volume Data. <https://www.sisweb.com/index/referenc/tenaxta.htm>.
52. Güntner, A. T., Magro, L., van den Broek, J. & Pratsinis, S. E. Detecting methanol in hand sanitizers. *iScience* **24**, 102050 (2021).
53. Abegg, S., Magro, L., van den Broek, J., Pratsinis, S. E. & Güntner, A. T. A pocket-sized device enables detection of methanol adulteration in alcoholic beverages. *Nat Food* **1**, 351–354 (2020).
54. Maier, I. & Fieber, M. Retention characteristics of volatile compounds on tenax TA. *J High Resolut Chromatogr* **11**, 556–576 (1988).
55. van den Broek, J., Mochalski, P., Königstein, K., Ting, W. C., Unterkofler, K., Schmidt-Trucksäss, A., Mayhew, C. A., Güntner, A. T. & Pratsinis, S. E. Selective monitoring of breath isoprene by a portable detector during exercise and at rest. *Sens Actuators B Chem* **357**, (2022).
56. Drabinska, N., Flynn, C., Ratcliffe, N., Belluomo, I., Myridakis, A., Gould, O., Fois, M., Smart, A., Devine, T. & de Lacy Costello, B. P. J. A literature survey of volatiles from the healthy human breath and bodily fluids: the human volatilome. *J Breath Res* **14**, 34001 (2021).
57. Güntner, A. T., Pineau, N. J. & Pratsinis, S. E. Flame-made chemoresistive gas sensors and devices. *Prog Energy Combust Sci* **90**, (2022).
58. Anderson, J. C. Measuring Breath Acetone for Monitoring Fat Loss: Review. *Obesity* **23**, 2327–2334 (2015).
59. Bessonneau, V. & Thomas, O. Assessment of exposure to alcohol vapor from alcohol-based hand rubs. *Int. J. Environ. Res. Public Health* **9**, 868–879 (2012).

60. Frankel, M., Bekö, G., Timm, M., Gustavsen, S., Hansen, E. W. & Madsen, A. M. Seasonal variations of indoor microbial exposures and their relation to temperature, relative humidity, and air exchange rate. *Appl Environ Microbiol* **78**, 8289–8297 (2012).
61. Ferrus, L., Guenard, H., Vardon, G. & Varene, P. Respiratory Water Loss. *Respir Physiol* **39**, 367–381 (1980).
62. Huang, J., Kumar, S. & Hanna, G. B. Investigation of C3-C10 aldehydes in the exhaled breath of healthy subjects using selected ion flow tube-mass spectrometry (SIFT-MS). *J Breath Res* **8**, 037104 (2014).
63. Issitt, T., Wiggins, L., Veysey, M., Sweeney, S. T., Brackenbury, W. J. & Redeker, K. Volatile compounds in human breath: Critical review and meta-analysis. *J Breath Res* **16**, 024001 (2022).
64. Anderson, J. C., Babb, A. L. & Hlastala, M. P. Modeling Soluble Gas Exchange in the Airways and Alveoli. *Ann Biomed Eng* **31**, 1402–1422 (2003).
65. Murgia, A., Ahmed, Y., Sweeney, K., Nicholson-Scott, L., Arthur, K., Allsworth, M., Boyle, B., Gandelman, O., Smolinska, A. & Ferrandino, G. Breath-taking perspectives and preliminary data toward early detection of chronic liver diseases. *Biomedicines* **9**, (2021).

Figures

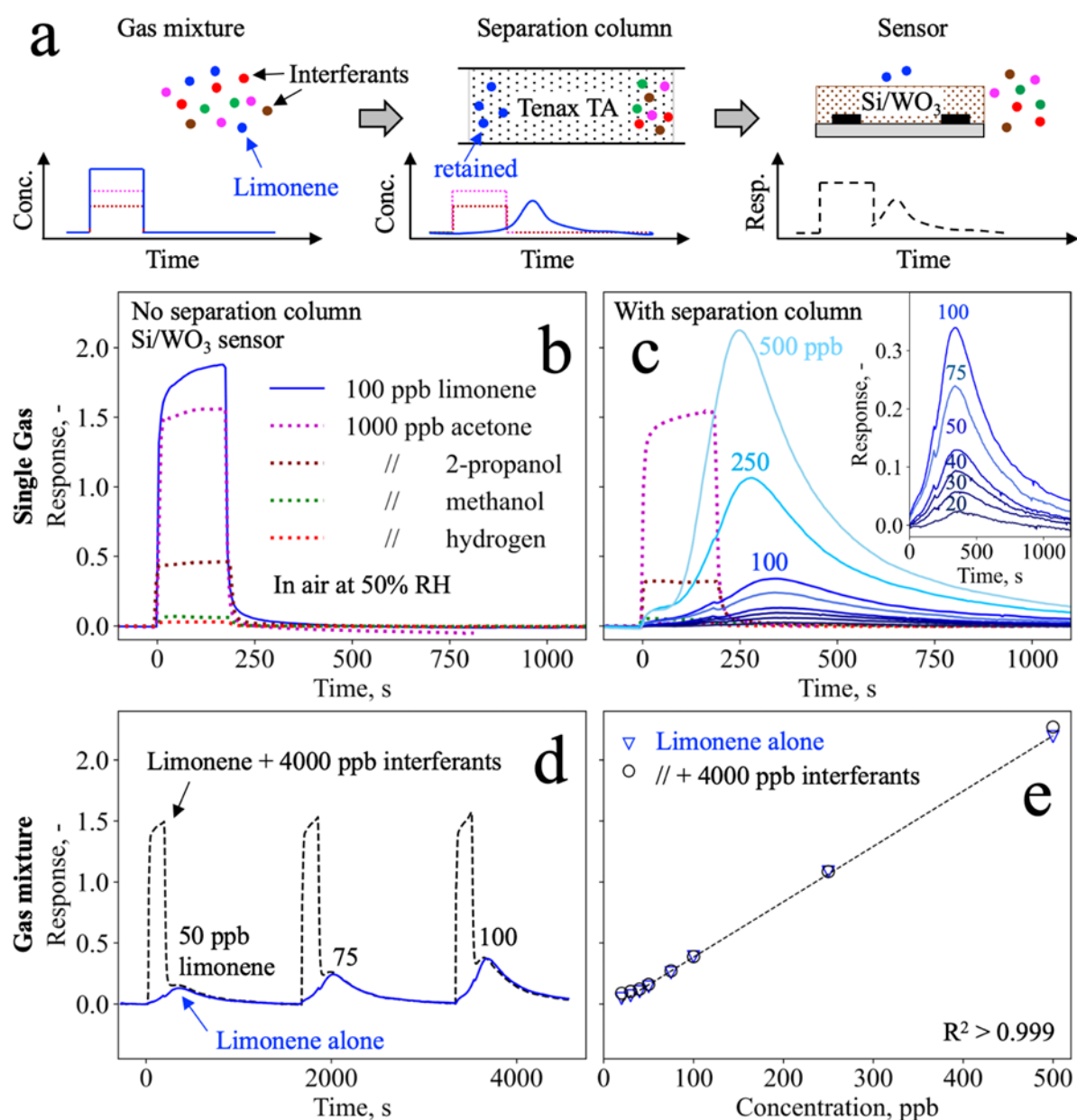


Figure 1: Selective ppb-level limonene sensing as single gas and in mixtures. (a) Concept illustration: Limonene is present in the complex chemical environment of exhaled breath. The separation column of Tenax particles retains limonene, while other volatiles referred to as interferants pass essentially unhindered. A chemoresistive sensor of Si/WO₃ nanoparticles placed downstream quantifies interferants and limonene sequentially, and thus, high selectivity is achieved. Si/WO₃ sensor response to 100 ppb limonene (blue, solid line) and to 1000 ppb acetone (purple, dotted line), 2-propanol (brown), methanol (green), and hydrogen (red) as single analytes (b) without and (c) with the Tenax separation column. Limonene concentrations between 20 and 500 ppb together with a magnification as inset in (c). (d) Si/WO₃ sensor response with separation column when exposed subsequently to 50, 75 and 100 ppb limonene alone (solid line) and for limonene in a gas mixture (dashed line) with the interferants methanol, 2-propanol, hydrogen and acetone, each at 1000 ppb. (e) Respective response to 20 – 500 ppb limonene alone (triangles) and together with the same gas mixture (circles). All measurements are performed in air at 50% RH.

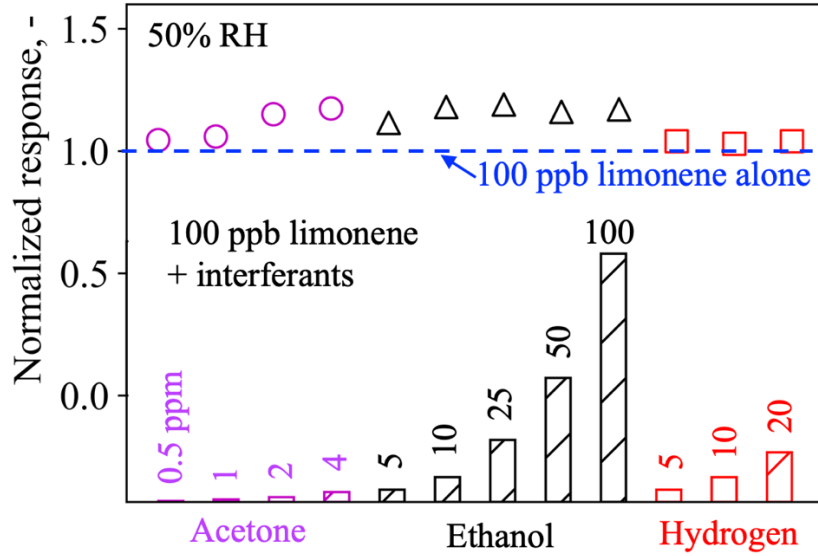


Figure 2: Normalized detector response to 100 ppb limonene in gas mixtures with 0.5 – 4 ppm acetone (purple bars and circles), 5 – 100 ppm ethanol (black bars and triangles), and 5 – 20 ppm hydrogen (red bars and squares) at 50% RH. The detector response is normalized to the response to 100 ppb limonene alone (dashed blue line).

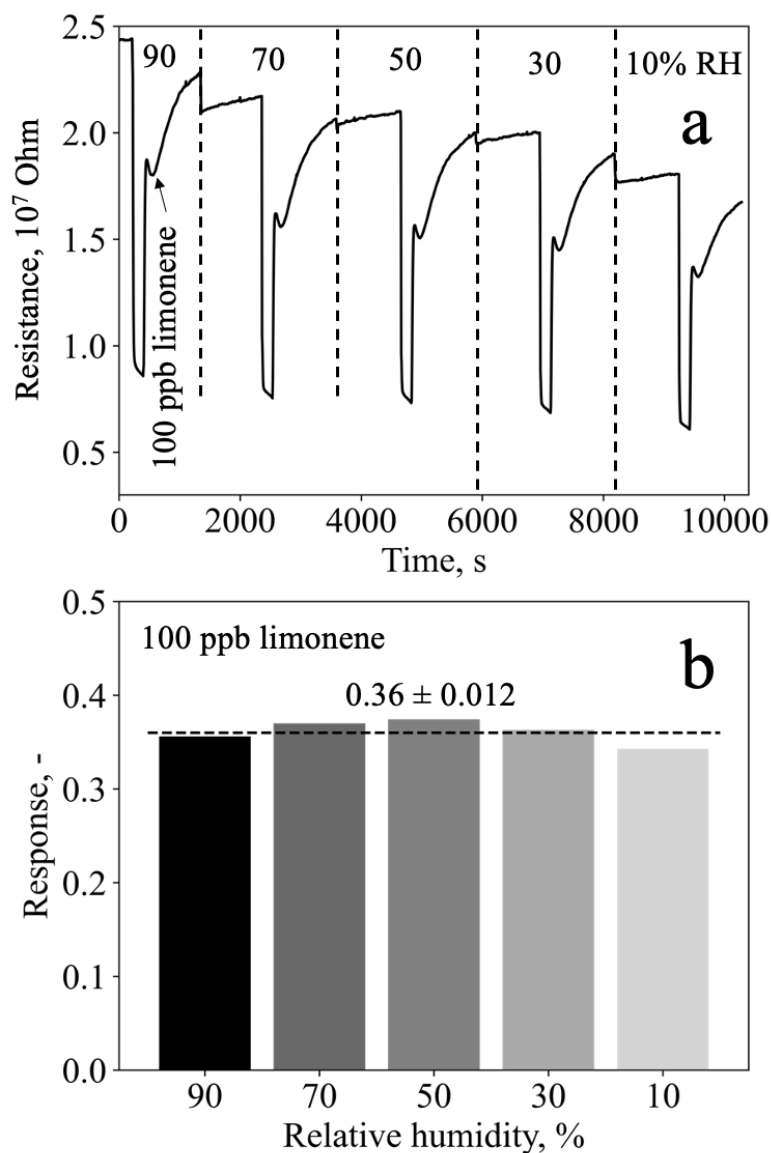


Figure 3: Humidity robustness. (a) Detector resistance upon exposure to 100 ppb limonene together with a gas mixture of 1000 ppb acetone at 90% RH, or with a total of 4000 ppb interferants, i.e., methanol, 2-propanol, hydrogen and acetone, each at 1000 ppb, at 70, 50, 30 and 10% RH. Note that at 90% RH, only 1000 ppb acetone is used due to a limitation of the measurement setup. **(b)** Corresponding detector responses for 100 ppb limonene as a function of RH. The average limonene response (dashed line) and standard deviation are shown, indicating that the detector response is hardly altered by RH at 10 – 90% in the presence of interferants.

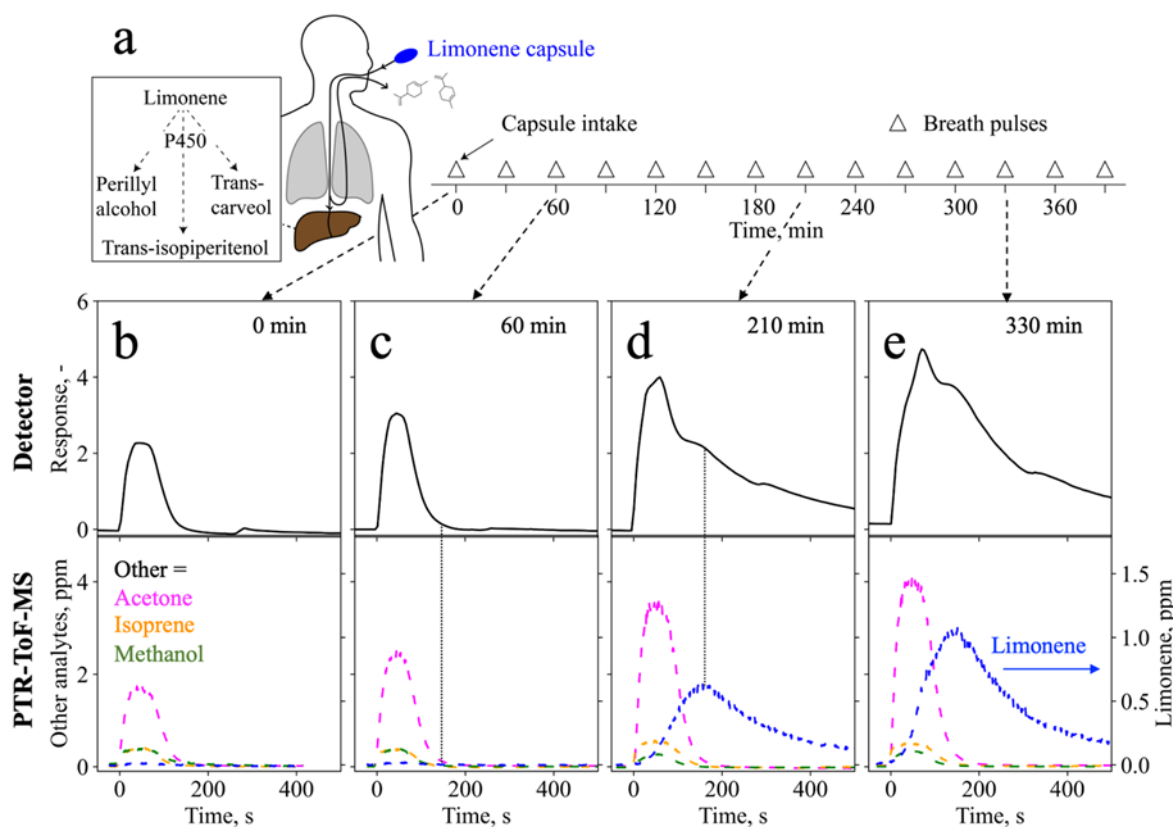


Figure 4: Breath measurements. (a) After the consumption of a limonene capsule at time = 0 min, limonene passes through the gut and is released to breath either directly through the oesophagus or through the diffusive exchange from blood in the lung alveoli.⁶⁴ When it reaches the liver through the blood circulation, limonene is metabolized to perillyl alcohol, trans-carveol, and trans-isopiperitenol by cytochrome P450 enzymes.¹⁶ Unmetabolized limonene diffuses from the blood to the breath, where it is analysed every 30 min for volunteer #1, as indicated by the triangles. Detector response (black solid line, top) and corresponding PTR-ToF-MS concentrations (dashed lines, bottom) of acetone (purple, left ordinate), isoprene (orange), methanol (green) and limonene (blue, right ordinate) (b) before ingestion of the capsule and (c) 60 min, (d) 210 min, and (e) 330 min after ingestion of the capsule (all other time points can be seen in Figure S6). Note that the breath exposure times (30 s exhalation + 54 s buffering inside end-tidal sampler³⁷), and thus the limonene retention time (see Figure S4), are shorter compared to those shown in Figures 1 and 3.

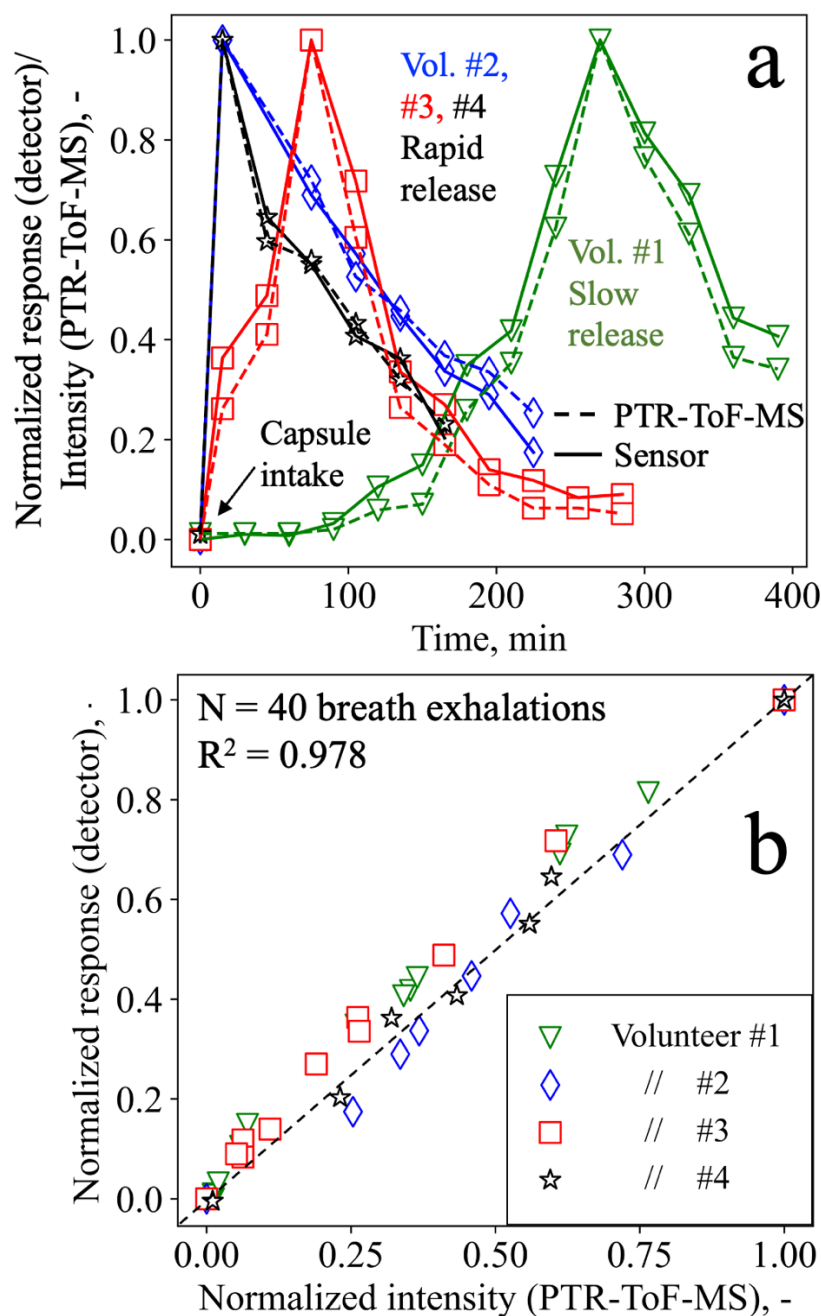


Figure 5: Dynamic limonene monitoring. (a) Normalized breath limonene intensities of volunteers #1 (triangles), #2 (diamonds), #3 (squares) and #4 (stars) as measured by the detector (solid line) and the PTR-ToF-MS (dashed line) as a function of time. Note that volunteers #2, #3 and #4 chewed the capsule to trigger a faster limonene release, while #1 swallowed it whole, resulting in a slow release in the gut. (b) Scatter plot showing the normalized limonene levels of all volunteers (sample size N = 40) as detected with the PTR-ToF-MS and the detector.

ToC graphic

